Relative Changes of Cerebral Arterial and Venous Blood Volumes During Increased Cerebral Blood Flow: Implications for BOLD fMRI

Sang-Pil Lee,[1] Timothy Q. Duong,[1] Guang Yang,[2] Costantino Iadecola,[2] and Seong-Gi Kim[1*]

Measurement of cerebral arterial and venous blood volumes during increased cerebral blood flow can provide important information regarding hemodynamic regulation under normal, pathological, and neuronally active conditions. In particular, the change in venous blood volume induced by neural activity is one critical component of the blood oxygenation level-dependent (BOLD) signal because BOLD contrast is dependent only on venous blood, not arterial blood. Thus, relative venous and arterial blood volume (rCBV) and cerebral blood flow (rCBF) in α-chlorolase-anesthetized rats under hypercapnia were measured by novel diffusion-weighted ^{19}F NMR following an i.v. administration of intravascular tracer, perfluorocarbons, and continuous arterial spin labeling methods, respectively. The relationship between rCBF and total rCBV during hypercapnia was $rCBV(total) = rCBF^{0.40}$, which is consistent with previous PET measurement in monkeys. This relationship can be linearized in a CBF range of 50–130 ml/100 g/min as $\Delta rCBV(total)/\Delta rCBF = 0.31$ where ΔrCBV and ΔrCBF represent rCBV and rCBF changes. The average arterial volume fraction was 0.25 at a basal condition with CBF of ~60 ml/100 g/min and increased up to 0.4 during hypercapnia. The change in venous rCBV was 2-fold smaller than that of total rCBV ($\Delta rCBV(vein)/\Delta rCBF = 0.15$), while the arterial rCBV change was 2.5 times larger than that of total rCBV ($\Delta rCBV(artery)/\Delta rCBF = 0.79$). These NMR results were confirmed by vessel diameter measurements with in vivo videomicroscopy. The absolute venous blood volume change contributes up to 36% of the total blood volume change during hypercapnia. Our findings provide a quantitative physiological model of BOLD contrast. Magn Reson Med 45:791–800, 2001.

Key words: CBV; CBF; BOLD; diffusion; hypercapnia; ^{19}F NMR; arterial spin labeling; brain

Cerebral arterial and venous blood volumes (CBV) are important indicators of brain tissue physiology, viability, and function. Measurement of the arterial and venous CBV in vivo can provide valuable information regarding hemodynamic regulation under normal and pathological conditions. In addition, measurements of arterial and venous CBV changes during increased cerebral blood flow (CBF) can provide insight into the mechanism of blood oxygenation level-dependent (BOLD) contrast, commonly used for functional brain mapping (1). BOLD signals are modulated by changes in *venous*, not arterial, blood volume because venous blood contains paramagnetic deoxyhemoglobin which dephases NMR signals as a result of its difference in susceptibility from surrounding tissue. On the other hand, arterial blood that contains diamagnetic oxyhemoglobin does not contribute significantly to BOLD signals (2,3). Therefore, separation of the blood volume contribution from the arterial and venous sides of the vascular system is crucial to quantify BOLD signals.

CBV has been measured in vivo using various intravascular contrast agents with NMR (e.g., iron-oxide compounds and Gd-DTPA) (4–8) and using intravascular radioactive tracers with positron emission tomography (PET) (9,10) and computed tomography (11). Although the volume change of the entire vascular system (including both arterial and venous blood) can be measured, arterial and venous blood volumes cannot be separated by these methodologies. Nevertheless, it has been proposed that the change in venous blood volume dominates the total CBV change during altered CBF by neural stimulation and hypercapnia (8,12). However, this assumption is questionable since small arterioles are known to dilate during increased CBF (13–15).

Recently, this laboratory developed a regional arterial and venous CBV fraction measurement method using a diffusion-weighted ^{19}F NMR method following i.v. administration of perfluorocarbon (PFC) (16). Diffusion-weighted NMR signals of intravascular PFC show two distinct pseudo-diffusion (D*) components: one a fast-moving component, the other a slow-moving component. It has been demonstrated that the larger D* component predominantly reflects more oxygenated arterial blood, while a smaller D* component represents less oxygenated venous blood (16). Thus, diffusion-weighted ^{19}F NMR can be used to separately measure the volume fractions of arterial and venous blood.

Here, this ^{19}F diffusion methodology was further employed to investigate the modulation of arterial and venous CBV during hypercapnia-induced CBF change. Relative arterial and venous CBV (rCBV) were determined by diffusion-weighted ^{19}F NMR, while relative CBF (rCBF) was measured using a two-coil continuous arterial spin labeling method (17). To correlate our NMR results, changes in arterial and venous vessel diameters induced by hypercapnia were also measured by in vivo optical microscopy (14).

THEORY

Since the details of the arterial and venous blood volume fraction measurement method were described previously

[1]Center for Magnetic Resonance Research, Department of Radiology, University of Minnesota Medical School, Minneapolis, MN.

[2]Laboratory of Cerebrovascular Biology and Stroke, Department of Neurology, University of Minnesota Medical School, Minneapolis, MN.

Grant sponsor: National Institutes of Health; Grant numbers: RR08079; NS38295; NS38252; Grant sponsor: Keck Foundation.

*Correspondence to: Seong-Gi Kim, Ph.D., Center for Magnetic Resonance Research, Department of Radiology, University of Minnesota Medical School, 2021 Sixth Street SE, Minneapolis, MN 55455. E-mail: kim@cmrr.umn.edu

Received 24 July 2000; revised 1 November 2000; accepted 14 November 2000

(16), only a brief summary is included here. PFC emulsions are excellent blood substitutes and NMR-detectable. When PFCs are administered into blood, they do not cross the blood–brain barrier, and, thus, are reliable intravascular NMR tracers.

The cerebral vasculature can be modeled as two nonexchanging compartments, namely, an arterial and a venous pool. It is assumed that the capillary volume is small and/or the contribution is distributed to arterial and venous components. To examine intravascular blood motion, diffusion-weighted ^{19}F NMR can be used. According to the intravoxel incoherent motion (IVIM) model (18), the diffusion-weighted signal from two nonexchanging compartments with randomly oriented blood vessels can be described as:

$$\frac{S_b}{S_0} = f \cdot e^{-TE \cdot R_{2(1)}} \cdot e^{-b \cdot D_1^*} + (1 - f) \cdot e^{-TE \cdot R_{2(2)}} \cdot e^{-b \cdot D_2^*}, \quad [1]$$

where S_b and S_o are the signal intensities obtained at diffusion-weighting factors of b and 0, f is the fraction of spins with a large pseudo-diffusion coefficient, TE is the echo time, $R_{2(1)}$ and $R_{2(2)}$ are the transverse relaxation rates of the fast- and slow-moving components, and D_1^* and D_2^* are the pseudo-diffusion coefficients of fast- and slow-moving spins, respectively. Assuming rectangular-shaped gradient pulses, the diffusion weighting factor, b, can be expressed as (19):

$$b = (\gamma \cdot \delta \cdot G)^2(\Delta - \delta/3), \quad [2]$$

where γ is the gyromagnetic ratio of nuclei, G is a bipolar gradient strength, Δ is the inter-gradient separation, and δ is the gradient duration.

Assuming $R_{2(1)}$ and $R_{2(2)}$ are the same, Eq. [1] can be rewritten as:

$$S_b/S_0 = f \cdot \exp(-b \cdot D_1^*) + (1 - f) \cdot \exp(-b \cdot D_2^*). \quad [3]$$

In this case, f can be easily determined by fitting diffusion-weighted NMR data using Eq. [3]. Previous studies showed that two pseudo-diffusion coefficients exist in vivo; D_1^* is approximately 80 times greater than D_2^*, and f is about 0.3 in a normocapnic condition (16,20). This biexponential characteristic disappeared when animals were sacrificed (16).

Since dissolved O_2 is an effective longitudinal relaxation agent of ^{19}F in blood, the spin-lattice relaxation rate (R_1) of ^{19}F is linearly correlated with dissolved oxygen concentration. Thus, PFCs in blood have two distinct longitudinal relaxation time constants (T_1), the shorter T_1 associated with fully oxygenated arterial blood, and the longer T_1 associated with less oxygenated venous blood. To determine whether the D_1^* component is related to the shorter T_1 of arterial blood, inversion recovery experiments were combined with a diffusion-weighting method, previously described in detail (16). At each inversion recovery time, the fraction of spins, f, with a large pseudo-diffusion coefficient, D_1^*, was determined by fitting diffusion-weighted ^{19}F NMR data from the rat brain using Eq. [3]. Figure 1 shows the fraction of the fast-moving component in diffusion-weighted ^{19}F NMR as a function of inversion time (TI). The fraction of the fast moving component decreased to almost 0% when TI was ~0.28 sec, whereas it became 100% when TI was ~0.49 sec. This result demonstrates that the fast-moving D_1^* component is associated with a shorter T_1 (oxygenated arterial blood), while the slow-moving D_2^* component is associated with a longer T_1 (less-oxygenated venous blood). Thus, the diffusion-weighting method can provide arterial and venous blood volume fractions.

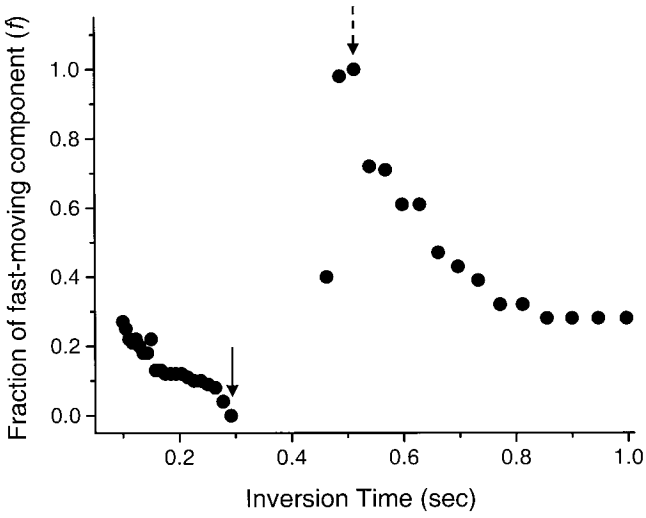

FIG. 1. Cerebral blood volume fractions of the fast-moving component (f) in diffusion-weighted experiments in a representative rat at various inversion times. Inversion time was varied to selectively null one T_1 constituent in two, nonexchanging T_1 components. Based on the dependence of T_1 on blood oxygenation level (16), the short T_1 component is associated with arterial blood, while the long T_1 component is associated with venous blood. The fraction of the fast-moving arterial component became almost zero at TI = 0.28 sec, which nulls arterial blood, and 1.0 at TI = 0.49 sec, which nulls venous blood. At very short and long inversion times, f ($\equiv f_a$) was about 0.25.

MATERIALS AND METHODS

NMR Studies

Perfluorocarbon

The effect of PFC as a blood substitute on an in vivo system has been extensively studied and reviewed (21,22). No significant disturbance in living systems has been reported and some PFCs are approved for use in human studies. The perfluoro-15-crown-5-ether (Exfluor Research Corp., Round Rock, TX) emulsion used in this experiment has been successfully used in mice and rats without detrimental effects (23). Unlike other PFC compounds, perfluoro-15-crown-5-ether has a single resonance peak from 20 equivalent ^{19}F atoms, resulting in high sensitivity. Since the PFC is not water soluble, it was emulsified into ~200-nm diameter micelles (40% v/v; Gateway Technology, St. Louis, MO). The mean half-life of PFC in the blood stream is expected to be 2 days (22).

To determine the relationship between oxygen tension and ^{19}F R_2, the T_2 of PFC in blood was measured by using

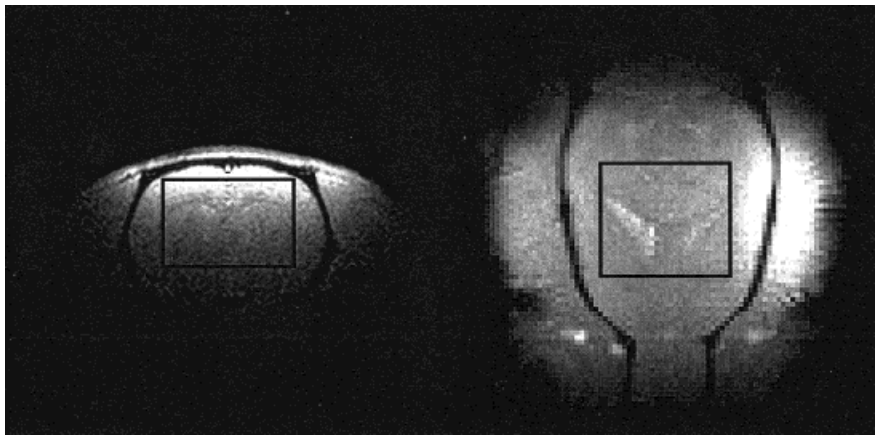

FIG. 2. Anatomical images with a region of interest used in all NMR measurements. Coronal (left) and axial (right) slices are shown. Imaging parameters for FLASH sequence were TE/TR of 5 msec/10 msec, slice thickness of 1 mm, and flip angle of 16°. The size of the ROI was $9 \times 6 \times 8$ mm^3.

a double spin-echo spectroscopy technique. The oxygen tension and oxygenation level of the blood were varied by bubbling the specimen with a mixture of oxygen and nitrogen gases with different oxygen concentrations at room temperature (20°C). Blood oxygenation and blood oxygen tension were measured using a blood gas analyzer (Chiron Diagnostics, Norwood, MA). R_2 data were fitted as functions of hemoglobin oxygenation level (Y) and dissolved oxygen tension (pO_2) by using a multiple regression method (with a hemoglobin dissociation curve at pH of 7.4).

Animal Preparation

Sprague-Dawley rats weighing 200–275 g were anesthetized with 2% isoflurane (Marsam Pharmaceutics, Cherry Hill, NJ) in a 1:1 mixture of N_2O and O_2 during surgical procedures. Catheters were inserted into the left femoral artery and the femoral vein to measure arterial blood pressure and arterial blood gases and to deliver drugs, respectively. Arterial blood pressure and breathing pattern were recorded with a multitrace recorder (AcqKnowledge; Biopac Systems, Santa Barbara, CA). Mean arterial blood pressure was 105 ± 10 mmHg. End tidal CO_2 concentration and inspired O_2 concentration were continuously monitored with a capnometer (SC-300; BCI International, Waukesha, WI) and an oxygen sensor (Kent Scientific, Litchfield, CT).

After surgery, isoflurane anesthesia was switched to α-chloralose, which was administered through the femoral vein. The α-chloralose was initially administered as an 80-mg/kg bolus and continuously infused afterwards at 26.7 mg/kg/hr. The head of the animal was secured in a head holder by means of ear pieces and a bite bar. Before NMR measurements, at least 1–2 hr were allowed for stabilization of the animal and clearance of isoflurane after switching anesthesia to α-chloralose. Body temperature was maintained throughout the measurements at 37 ± 0.5°C by means of a temperature-controlled water blanket. The pH-balanced, isotonic PFC emulsion was administered intravenously (10–12 ml/kg) without withdrawing any blood.

To induce graded hypercapnic conditions, CO_2 gas was added to the breathing gas mixture by substituting a volume of N_2O gas with the equivalent volume of CO_2 gas (up to 9%) and leaving the inspired O_2 tension unperturbed. Mechanical ventilation parameters (e.g., breathing rate, volume) were kept constant.

NMR Methods

All NMR measurements were performed on a 9.4 T, 31-cm diameter horizontal magnet (Magnex Scientific, Abingdon, UK), equipped with an actively shielded, 11-cm inner diameter gradient-insert operating at maximum gradient strength of 30 G/cm and a rise time of 300 μs (Magnex Scientific), interfaced to a Unity INOVA console (Varian, Palo Alto, CA). Experiments were conducted with a home-built RF coil (o.d. = 1.2 cm) which is actively tunable to ^{1}H (400 MHz) or ^{19}F frequency (376 MHz) by employing both a PIN diode and a variable capacitor in parallel to the RF coil (24). The capacitor serially connected to the PIN diode was adjusted to the separation of the two frequencies. When a PIN diode was reverse-biased, it worked as a capacitor whose capacitance was ~2.5 pF. With this setup, the RF coil was tuned to the ^{19}F frequency. On the contrary, when the PIN diode was forward-biased it functioned as a short circuit with very little stray capacitance. The switchable RF coil was positioned on top of the rat head for ^{19}F and ^{1}H RF excitation and detection and a butterfly-shaped surface coil (0.5 cm diameter) was placed under the neck for arterial spin labeling.

Multislice FLASH images were acquired to identify anatomical structures in the brain and to position the region of interest at the isocenter of the magnetic field. Magnetic field homogeneity was optimized by volume localized shimming (FASTMAP) (25) to yield a water spectral line width of 16–24 Hz on a typical $9 \times 7 \times 8$ mm^3 voxel located in the brain without noncerebral tissue contamination (Fig. 2). A volume-localized STEAM sequence with ultrashort echo-time (26) was used for interleaved ^{19}F and ^{1}H studies.

Total rCBV and CBF Measurements

In order to measure relative CBV and CBF changes, ^{19}F and ^{1}H spectra were acquired in an interleaved manner while the inhaled CO_2 concentration in the gas mixture was gradually increased up to 9%. Eight scans of ^{19}F NMR spectra were averaged for CBV measurements and four ^{1}H

spectra were averaged for CBF measurements using the continuous arterial spin labeling method. Temporal resolution of both ^1H and ^{19}F NMR measurements was typically 120 sec.

Since the total CBV is directly related to the spin density (M_o) of PFC in blood, in vivo volume-localized ^{19}F NMR spectra were obtained at two or three echo times (TE = 2.2, 7, and 15 msec or TE = 2.2 and 8 msec) with a long repetition time ($\sim 5T_1$ = 4 sec). Line broadening of 20 Hz was applied before Fourier transformation and integration of the spectra were performed. M_o was estimated by two methods: extrapolation from a least-squares fit of multiple echo-time data and estimation from the NMR data with the shortest echo time of 2.2 msec. Because the two methods yielded almost identical results, M_o obtained from the shortest echo-time data was used (due to less signal fluctuation) for further data analysis. Relative CBV was determined by normalizing with the spin density at normocapnia.

For continuous arterial spin labeling, a 3-sec long rectangular RF pulse was applied to the neck coil (17,27). The power of the labeling RF pulse was adjusted to maximize the degree of spin labeling (α) in each animal. Control and labeled spectra were obtained alternately by switching the sign of the frequency offset. Assuming the effect of macromolecules is negligible, CBF values were calculated in units of ml/g tissue/sec using:

$$CBF = \frac{\lambda}{T_1} \frac{S_C - S_L}{S_L + (2\alpha - 1)S_C}, \quad [4]$$

where λ is the blood–brain partition coefficient of water, T_1 is the tissue water spin-lattice relaxation time, and S_C and S_L are signal intensities of control and arterial spin labeling periods, respectively. The values used for the calculation were λ of 0.9 (28), T_1 of 1.9 sec, and α of 0.62–0.75 obtained from high-resolution FLASH images acquired during arterial spin labeling (17,29).

Arterial and Venous CBV Fraction Measurements

Interleaved measurements of CBF and arterial/venous CBV were performed on six rats. Three to four hypercapnic conditions were used for each animal. At least 20 min were allowed for CBF values to reach equilibrium after changing CO_2 conditions. During waiting periods, CBF was continuously measured to ensure the steady-state condition. For arterial/venous CBV fraction measurements, typical parameters were TE = 9 msec, Δ = 15 msec, δ = 4 msec, and G up to 25 G/cm. Eleven logarithmically spaced *b* values, 0, 3, 6, 12, 25, 50, 100, 200, 500, 800, and 1200 sec/mm^2, were used. The orders of the *b* values were randomized to minimize potential systematic errors. Since arterial and venous blood have different T_1 values, a sufficiently long delay time ($\sim 5T_1$) was used to avoid uneven T_1 weighting effects on two different components. To obtain a sufficiently high SNR with diffusion-weighted spectra, 32 transients were averaged for ~24 min. Exponential apodization (20 Hz of line broadening) was applied before Fourier transformation. The signal intensities of the spectra were used for biexponential curve-fitting to Eq. [3] (Origin; Microcal, Northampton, MA). Pseudo-diffusion coefficients and the fraction of arterial blood component were determined.

Artery and Vein Diameter Measurements

To validate our NMR measurements of relative arterial and venous CBV changes during hypercapnia, diameters of arteries and veins were measured in vivo using methods described in detail previously (14). A different group of Sprague Dawley rats (275–300 g; n = 8) were initially anesthetized with 5% halothane in 100% oxygen and maintained with 1–2% halothane. A small cranial window (3×3 mm^2) was produced in the interparietal bone and then continuously superfused with Ringer solution equilibrated with 95% O_2 and 5% CO_2 (pH 7.3–7.4). Diameters of pial vessels in cerebellar cortex were measured with a microscope placed directly above the cranial window. Images of vessels were obtained with a video camera (Panasonic, Japan). Vascular diameter was measured with a calibrated video microscaler (Optech, Trenton, NJ). Arterioles could be easily distinguished from venules on the basis of bright red blood color, fast red blood cell flow, and thicker vessel walls.

RESULTS

T_2 of PFC in Blood

The R_2 of ^{19}F in blood at various oxygen concentrations in vitro is shown in Fig. 3. Shaded areas indicate typical ranges of venous blood oxygenation and arterial oxygen tension in our in vivo experimental condition (3). The R_2 of PFC in blood was influenced not only by dissolved oxygen but also by the concentration of paramagnetic deoxyhemoglobin. When the oxygen saturation of hemoglobin is less than ~0.98, such as in venous blood, the R_2 of PFC is negatively correlated with the blood oxygenation (Y), as shown in Fig. 3a. This suggests that deoxyhemoglobin is a dominant relaxation agent compared to the dissolved oxygen in blood at 9.4 T. At a higher blood oxygenation level, such as in arterial blood, R_2 is positively correlated with the blood oxygen tension (pO_2), as shown in Fig. 3b. The difference in R_2 between arterial and venous blood can induce errors in determining arterial and venous volume fractions when Eq. [3] is used because it is assumed that T_2 values in the two pools are the same. Since T_2 of arterial blood is longer than that of venous blood, the arterial volume fraction ($f \equiv fa$) calculated using Eq. [3] is likely to be slightly overestimated. However, the R_2 difference of PFC in arterial and venous blood is not significant, resulting in less than 0.4% error in the *fa* measurement.

The in vivo T_2 of perfluorocarbon in the cerebral vasculature of α-chloralose anesthetized rats was also determined at 9.4 T. The value of T_2 in vivo was ~10 msec, which is much smaller than the in vitro T_2 of 200–300 msec of arterial and venous blood samples. The shortened T_2 can be attributed to the flow of blood in vivo, which can dephase ^{19}F transverse magnetization and result in the decrease of the apparent T_2. To confirm that the shortened T_2 is due to flow, the T_2 of PFC in a flow phantom with a mixture of pseudo-randomly orientated tubes was measured. When flow velocity increased, T_2 decreased dramat-

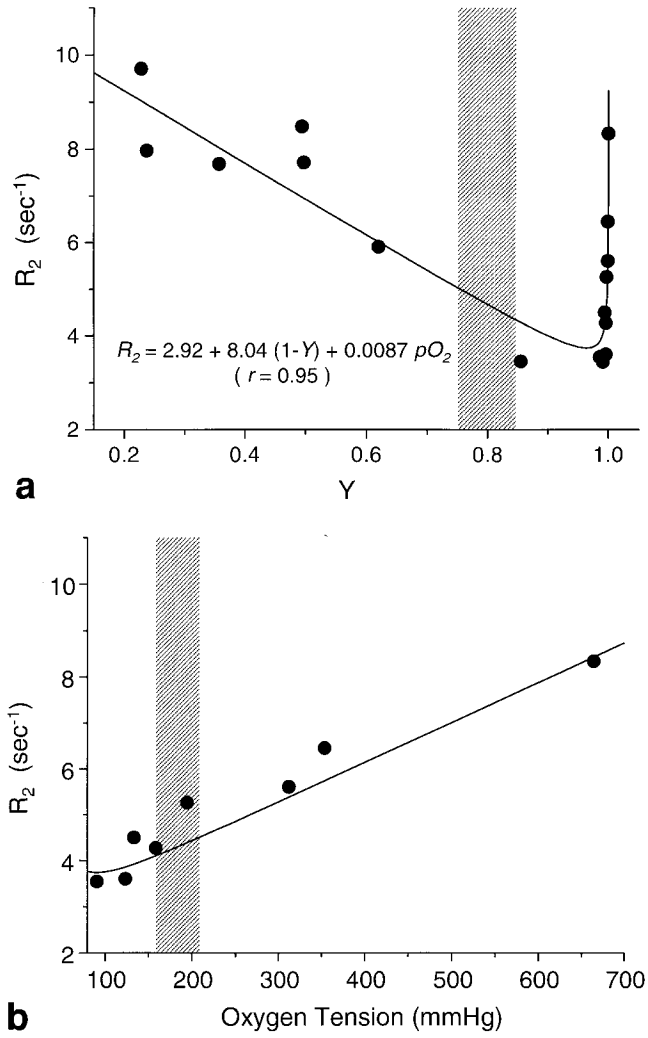

FIG. 3. Dependence of ^{19}F R_2 in blood on blood oxygenation level. Relationship between R_2 of ^{19}F and blood oxygenation (Y) is shown in **a**. Deoxyhemoglobin dominated the transverse relaxation of PFC until blood was fully oxygenated. Only when blood was fully oxygenated, the oxygen tension dependence of ^{19}F R_2 could be seen in **b**. Filled circles represent data acquired at room temperature (20°C). A solid line was obtained by fitting data as function of oxygenation level and dissolved oxygen pressure using a multiple regression method. Shaded areas are normal physiological ranges in our experimental condition.

ically, suggesting that flow is the major cause of short ^{19}F T_2 in vivo (data not shown).

Total rCBV and rCBF Relationship During Hypercapnia

After the PFC emulsion was infused into rats via the femoral vein, arterial mean blood pressure, heart rate, end-tidal CO_2, and blood gases were not significantly changed. Physiological parameters during normocapnic conditions were mean arterial blood pressure 100–110 mmHg, heart rate 400–430 BPM, pO_2 170–195 mmHg, pCO_2 36–42 mmHg, and pH 7.3–7.4.

Figure 4 shows total rCBV and rCBF changes of two animals during graded CO_2 gas inhalation. End-tidal CO_2 level increased from 4% during a normocapnic condition to 13% during inhalation of a 9% CO_2 gas mixture. Total rCBV and rCBF values were normalized by those measured during the normocapnic condition ($PaCO_2$ = 40 ± 2 mmHg), which corresponds to CBF of 58 ± 3 ml/100 g tissue/min. The relationship between rCBF and rCBV is $rCBV(total) = 0.97 \times rCBF^{0.40}$, and also can be expressed in a linear equation $rCBV(total) = 0.31 \times rCBF + 0.67$ (r = 0.85) in the range of the CBF between 40 and 130 ml/100 g/min. This implies that when rCBF increases 100%, total rCBV increases ~31%. This relationship between rCBF and rCBV is in good agreement with that determined by PET (9) and MRI with contrast agent (12).

Arterial and Venous rCBV Measurements

Eleven volume-localized diffusion-weighted ^{19}F spectra were acquired for arterial and venous CBV separation. Representative spectra obtained during a normocapnic condition are shown in Fig. 5a. Normalized diffusion-weighted ^{19}F NMR signals at three different CBF conditions in one representative animal are plotted in Fig. 5b. Clearly, biexponential signal decay characteristics were evident in two CBF conditions of 47 and 79 ml/100 g/min, while negligible signal decrease was observed postmortem. The pseudo-diffusion coefficient of PFC in blood was $\sim 1 \times 10^{-6}$ mm^2/sec postmortem. Pseudo-diffusion coefficients for the arterial and venous components were 40×10^{-3} and 0.28×10^{-3} mm^2/s at a CBF level of 47 ml/100 g/min, and 33×10^{-3} and 0.58×10^{-3} mm^2/s at a CBF level of 79 ml/100 g/min, respectively. Fitting errors of the D* given above were ~33% and ~14% for arterial and venous components, respectively. Due to the large fitting errors and the large inter-animal variations of D* values of arterial and venous blood, no statistically significant correlation between D* and CBF values was observed. The average values of D* coefficients over all animals were 43×10^{-3} mm^2/s in arterial blood and 0.57×10^{-3} mm^2/s

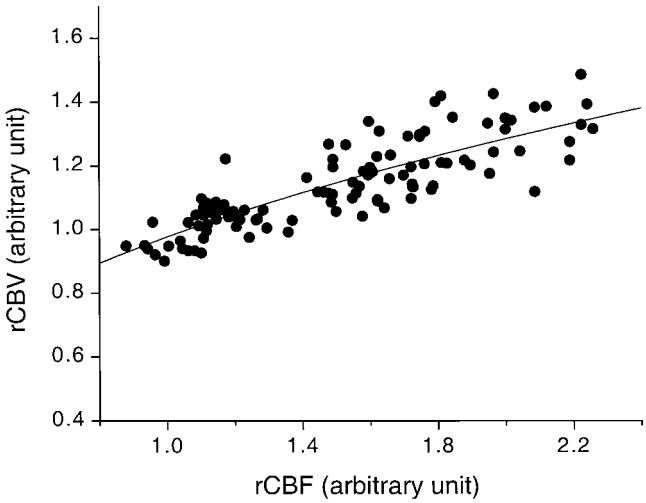

FIG. 4. Relationship between total rCBV and rCBF. Total CBV values were normalized with the CBV value at normocapnia (CBF = 58 ml/100 g/min). The relationship between rCBV and rCBF was fitted either in linear or in allometeric equations with almost identical chi-square values (sum of squared error) ($rCBV(total) = 0.97 \times rCBF^{0.4}$ or $rCBV(total) = 0.31 \times rCBF + 0.68$, r = 0.85, $P < 0.0001$).

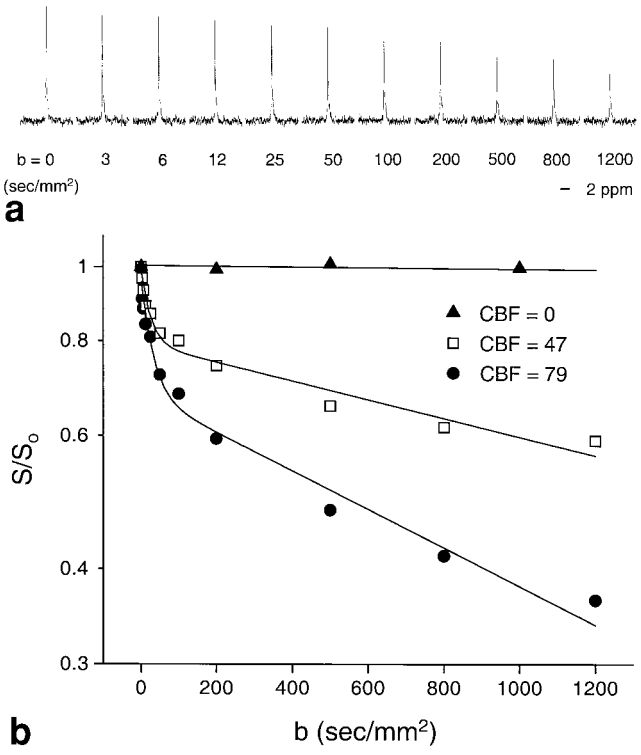

FIG. 5. **a:** Diffusion-weighted ^{19}F NMR spectra from the rat brain. Line broadening of 20 Hz was applied and the frequency range of each spectrum is 10 kHz. The critical velocity corresponding to the phase dispersion of $\pm\pi/2$ was 1.2 mm/sec for a *b*-value of 100 s/mm^2. **b:** Plots of the normalized signal intensities at three different CBF conditions (CBF = 0, 47, and 79 ml/100 g/min). Solid curves are least-square biexponential curve fits of live animal data. Pure diffusion of PFC was minimal based on the postmortem study.

in venous blood (a ratio of ~80), consistent with previous reports (16,20).

When CBF increased from 47 to 79 ml/100 g tissue/min, the arterial CBV fraction increased from 0.20 (with a fitting error of 0.02) to 0.29 (with a fitting error of 0.03) (Fig. 5b). All measured arterial blood volume fractions (f_a) in six animals are plotted in Fig. 6. Each animal contributed three to four data points corresponding to different hypercapnic conditions. A linear correlation between absolute CBF and f_a was observed ($f_a = 0.002 \times CBF + 0.137$, r = 0.7, $P < 0.001$).

The ^{19}F NMR signal intensity without diffusion-weighting obtained for arterial and venous CBV fraction measurements can provide total CBV if ^{19}F T_2 of blood remains constant. However, the T_2 of ^{19}F in venous blood increases when the venous oxygenation level elevates during hypercapnia (Fig. 3). Thus, total rCBV could not be directly determined from single-echo, diffusion-weighted ^{19}F spectra with a relatively long echo time (9 msec), which was necessary for incorporating diffusion gradients. Alternatively, total rCBV can be obtained from rCBF using the known relationship between rCBF and total rCBV (Fig. 4). Then arterial and venous rCBV can be separately determined using venous and arterial CBV fractions (Fig. 6). The relationship between arterial/venous rCBV and rCBF is shown in Fig. 7. Total rCBV and rCBF were normalized to those at a normocapnic condition (CBF = 58 ml/100 g tissue/min) in Fig. 7a, and arterial and venous rCBVs were normalized to their corresponding basal values for determining relative changes in Fig. 7b. Relative CBV data were block-averaged in a CBF range of 10 ml/100 g/min. Note that arterial and venous volume fractions during the normocapnic condition were 0.25 and 0.75, respectively (Fig. 7a). The arterial rCBV change was approximately 5.3 times of the venous rCBV change, as indicated by the slopes of the regression curves. Table 1 summarizes the results of linear regressions of rCBV and rCBF. A 100% increase in CBF results in 31% increase in total rCBV, 79% increase in arterial rCBV, and 15% increase in venous rCBV (Fig. 7b). When the fractional arterial and venous volume contributions were taken into account, the arterial CBV increase constituted 64% of total CBV increase while the venous CBV increase constituted 36% of the total CBV increase (Fig. 7a).

Artery/Vein Diameter Measurement During Hypercapnia

The diameter of small arterioles and venules was measured using in vivo videomicroscopy. Vascular structure data were grouped according to size (10–20 μm, 20–30 μm, and 30–40 μm). Figure 8 shows the fractional increase in the diameters of arterioles and venules during a hypercapnic condition (with an arterial pCO_2 increase from 34 to 54 mmHg). Smaller vessels showed larger diameter increases compared to larger vessels. More importantly, the diameter of arterioles changed more than that of venules. The average diameter increase of venous vessels with 10–30 μm diameter during hypercapnia was ~10%, while that of similar size arteries was ~50%. Assuming that the length of these vessels did not change, relative CBV in small vessels is directly proportional to the square of the vessel diameter. Thus, venous small vessel CBV increased by 11–23%, while arterial small vessel CBV increased by

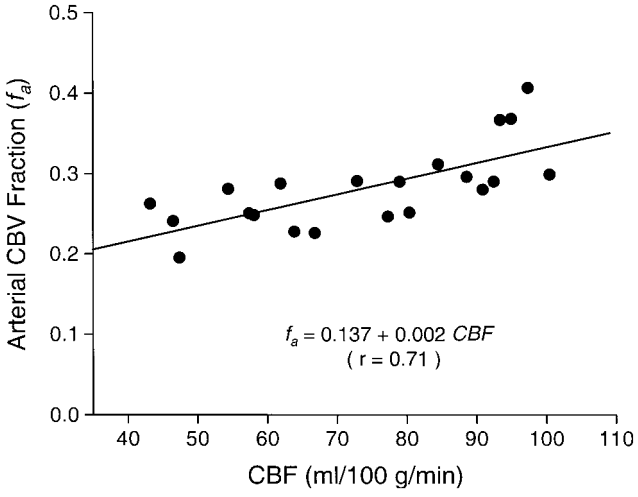

FIG. 6. The plot of the arterial blood volume fraction (f_a) vs. CBF measured by an arterial spin labeling method. Data are from six animals. Each animal contributed 3–4 data points from normocapnia to hypercapnia. A strong linear correlation between arterial CBV fraction and CBF was observed ($f_a = 0.002 \times CBF + 0.137$, r = 0.7, $P < 0.001$).

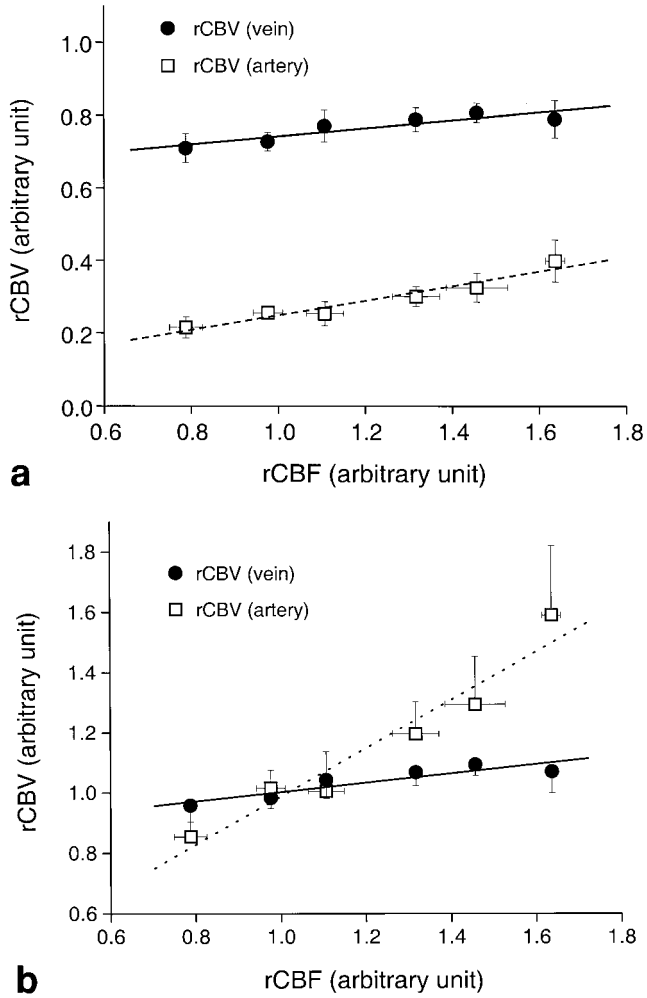

FIG. 7. Plots of venous and arterial rCBV vs. rCBF. **a:** Arterial and venous CBV values were obtained by multiplying arterial/venous blood volume fractions in Fig. 6 and total CBV changes in Fig. 4. Error bars indicate standard deviations of block averaged values of rCBVs and rCBF. Error bars on the rCBF axis are shown only in the rCBV(artery) trace. A solid line indicates the correlation of venous CBV and CBF ($rCBV(vein) = 0.11 \times rCBF + 0.63$, r = 0.9) and dotted line indicates that of arterial CBV and CBF ($rCBV(artery) = 0.20 \times rCBF + 0.05$, r = 0.97). Note that the sum of the slopes of both regression lines is 0.31, equivalent to the slope in Fig. 4 and the contribution of venous CBV changes to total rCBV change is ~36%. **b:** All rCBV and rCBV values were normalized to the corresponding values at normocapnia (CBF = 58 ml/100 g tissue/min) for better comparison. For visual clarity, one-sided error bars are displayed on the rCBV axis. Venous rCBV was linearly correlated with CBF ($rCBV(vein) = 0.15 \times rCBF + 0.85$, r = 0.90, $P = 0.014$). Linear correlation between arterial rCBV and CBF ($rCBV(artery) = 0.79 \times CBF + 0.19$, r = 0.97, $P < 0.002$) was observed. The slope of the regression line of arterial rCBV was ~5.3 times that of venous rCBV.

43–150% in three groups of vessels. Thus, the ratio between the venous and arterial CBV increases ranged from 1:4 to 1:7.

DISCUSSION

Technical Considerations

The ^{19}F NMR method for measuring total rCBV is simple and model-free since the spin density of infused PFC reflects intravascular blood volume. Because no endogenous fluorinated compounds exist, subtraction and/or suppression of background NMR signals is not necessary in ^{19}F NMR. In comparison, other MRI methods using contrast agents rely on the relaxation properties of water, which is modulated by the concentration of contrast agents in the blood. The reduction of water T_1 and/or T_2 due to contrast agents in blood can be detected by T_1- and/or T_2-weighted MRI to measure CBV changes. For accurate measurements, it is important to acquire changes of NMR signals only from vascular regions, not from neighboring tissue. Unfortunately, relaxation-based techniques may contain NMR signals from both vessels and tissue depending on the applied NMR techniques. This results in potential errors in determining relative CBV. However, the limitation of the ^{19}F NMR technique is its lower SNR compared to other MRI approaches. The degree of substitution of blood by PFC determines the SNR, which is limited by total blood volume and the alteration of physiology following the blood substitution by PFC. Thus, it is difficult to determine CBV changes at high spatial resolution using ^{19}F NMR.

The basis of venous and arterial CBV fraction measurements is that the fast-moving component is mostly of arterial origin, whereas the slow-moving component is mostly of venous origin, and the capillary volume is absorbed into its arterial and venous constituents (16). This method has two potential errors in determining arterial and venous volume fractions. First, since the diffusion-weighting method may not distinguish arterial blood completely from relatively fast-moving venous blood, there is a possibility that arterial blood volume fraction measured with the diffusion-weighting method may have a contribution from the fast-moving venous blood component. If the venous blood contribution to the fast-moving arterial component is significant, the arterial blood volume fraction is overestimated and its change induced by hypercapnia is underestimated. However, as shown in the inversion-weighted diffusion experiment (Fig. 1), the fast- or slow-moving component can be selectively eliminated based on the T_1 difference. It should be noted that Fig. 4a in our previous article (16) was mislabeled; correct vertical scaling factors should be 12x, 4x, and 1x for inversion recovery spectra with TI of 0.49 sec, 0.28 sec, and $5T_1$, respectively. Taken together, the contamination of venous blood in the fast-moving blood pool is minimal. Second, the R_2 difference of PFCs in arterial and venous blood can induce errors. During normal arterial and venous blood oxygenation level conditions, typical in vitro $R_{2(1)}$ and $R_{2(2)}$ are 4.3 and 4.7 sec^{-1}, respectively. Since $R_{2(1)}$ and $R_{2(2)}$ cannot be determined separately in living animals, it is assumed that the difference of R_2 in arterial and venous blood due to oxygenation is the same in vitro and in vivo. In this case, f_a determined using Eq. [3] would be overestimated by up to 0.4% based on a simulation. When CBF increases due to hypercapnia, arterial oxygen tension does not change while venous oxygenation level increases (decreasing $R_{2(2)}$). Then the arterial volume fraction measured using Eq. [3] during hypercapnia would still be overestimated, but less than that during normocapnia. This results in the underestimation of arterial blood volume *change* and overestimation of venous blood volume *change* induced by hypercapnia. Overall, the arterial blood volume

Table 1
Linear Regression Coefficients for Venous/Arterial/Total CBV and CBF Relationships

	f_a vs. CBF[a]	rCBV(total) vs. rCBF[b]	rCBV(vein) vs. rCBF[c]	rCBV(artery) vs. rCBF[c]
Slope	0.0020	0.31	0.15	0.79
Intercept	0.14	0.68	0.85	0.19
r (P-value)	0.70 ($P < 0.001$)	0.85 ($P < 0.001$)	0.90 ($P = 0.014$)	0.97 ($P < 0.002$)

[a]All data points from six animals were pooled and analyzed with linear regression.
[b]Similar number of rCBV and rCBF pairs from two animals were pooled and analyzed with a linear regression.
[c]rCBVs were block averaged in the CBF range of 10 ml/100 g/min before the linear regression.

contribution to total blood volume *change* reported in this article provides a *lower limit*.

As an alternative to ^{19}F NMR, ^{1}H diffusion-weighted NMR methods can be used to separate arterial and venous blood components based on the difference in flow characteristics of arterial and venous blood if signals from tissue are suppressed sufficiently. Multiple inversion recovery can be used to suppress tissue water signal based on the T_1 difference between blood and tissue (30). T_1 difference between blood and tissue can be enhanced by the introduction of relaxation or contrast agents into the blood (31). Additionally, due to the high sensitivity of ^{1}H NMR, this method can provide an estimate of arterial and venous blood volume changes in localized areas using imaging approaches.

rCBV and CBF Relationship

CBF in the entire brain was 58 ± 3 ml/100 g/min during normocapnia, which seems to be slightly lower than the literature values (32). A likely reason for the discrepancy is a partial volume effect. The brain volume covers not only cortex but also other structures such as white matter and ventricular areas, where CBF values are significantly lower than that of the cerebral cortex (data not shown). When CBF was obtained from the somatosensory cortex, it was 70–90 ml/100 g/min, which agrees extremely well with literature values (33).

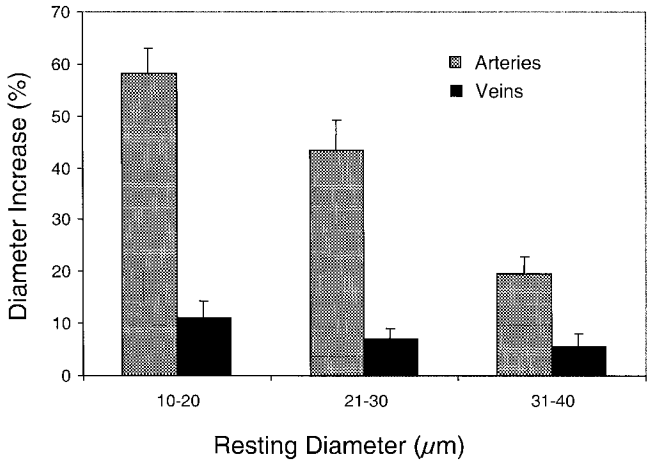

FIG. 8. Arterial and venous diameter changes produced by hypercapnia. Resting diameter (μm) represents vessel diameter at normocapnia. Data were averaged across eight animals and error bars = SEM.

The relationship between total rCBV and rCBF observed in the present study ($rCBV = rCBF^{0.40}$) agrees extremely well with previous measurements using PET in monkeys during hypercapnia ($rCBV = rCBF^{0.38}$) (9). In addition, the result is consistent with other NMR measurements using a contrast agent in the rat brain during forepaw stimulation (12).

Neil et al. (31) measured the change in the fast-moving component in diffusion-weighted ^{1}H spectra during hypercapnia. In their study, albumin-bound Gd-DTPA was used to reduce the T_1 of blood water. By utilizing large T_1 differences between tissue and blood water, blood signal can be predominantly obtained by selective nulling of tissue water using double inversion methods (30,31). Since the characteristics of blood flow is invariant regardless of probing methods, e.g., ^{19}F NMR with PFC or ^{1}H NMR with the selective suppression of tissue water signal, the fast-moving component in ^{1}H NMR results can be interpreted as the fast-moving arterial blood volume (16). The fast-moving component fraction measured by Neil et al. was about 0.25 at a pCO_2 level of 40 mmHg, and increased up to 0.45 in the hypercapnic condition (fig. 3 in Neil et al. (31)). These data are consistent with our arterial blood volume (fast-moving component) fraction changes during hypercapnia.

In our NMR studies, venous rCBV changes are much less than arterial rCBV changes. The ratio of arterial and venous rCBV changes measured by NMR is consistent with that determined by our vessel diameter measurements. It should be noted that vessel diameters were measured in the cerebellum under halothane anesthesia, while rCBV was measured in the cerebrum under α-chloralose anesthesia. It is known that hypercapnia similarly induces vascular diameter changes in the cerebrum and cerebellum (34). Furthermore, although the difference in anesthesia may affect vascular responses to hypercapnia, it is likely that the ratio between the diameter changes of arteries and veins will be preserved. Translation of the vessel diameter data into accurate rCBV change should take into account the fractional diameter change represented by all sizes of vessels and the distribution of these vessels. Thus, it is difficult to directly compare diameter change measured by videomicroscopy with rCBV measured by ^{19}F NMR. However, the ratio of arterial and venous rCBV changes in the entire brain measured by ^{19}F NMR can be compared with the ratio of arterial and venous diameter changes in small-size vessels measured by videomicroscopy, assuming large arterial and venous blood vessels behave similarly and also assuming that the ratios of blood volume fractions in

small and large vessels are similar in the arterial and venous trees.

Volume flow through blood vessels, which can be determined by the product of the cross section of the blood vessel (A) and the linear velocity (v), should be conserved at various sections of blood vessels. Thus, CBF can be changed by the modulation of A and/or v. Since the change of A is directly related to CBV, CBF and CBV changes are inter-related as $CBF_{stim}/CBF_{cont} = (A_{stim}/A_{cont}) \times (v_{stim}/v_{cont}) \approx (CBV_{stim}/CBV_{cont}) \times (v_{stim}/v_{cont})$, where subscripts "stim" and "cont" indicate "stimulated" and "control" conditions, respectively. According to our CBV and CBF observations during hypercapnia, it is expected that the increase of venous blood velocity is much more than that of arterial blood velocity considering that the rCBV change in venous blood is much less than that of arterial blood. An increase in blood velocity, especially in the venous blood pool, increases the dephasing of diffusion-weighted NMR signals, resulting in increased D* during hypercapnia. Neil et al. (31) demonstrated that D_1^* and D_2^* are linearly correlated with pCO_2 level, which is closely related to CBF. In our case, the D* values of arterial and venous blood did not show significant correlation with CBF due to a large variability between animals and trials. This needs to be further investigated.

The pseudo-diffusion coefficient (D*) is directly related to the pseudo mean-squared displacement ($\langle r^2 \rangle$), which is proportional to the square of velocity (35); $\langle r^2 \rangle \approx D^* \cdot \tau/6 \approx \langle (v \cdot \tau)^2 \rangle$, where v is the velocity of blood in the vessels and τ is the diffusion time. The average velocity of blood in various vascular sections can be estimated as 3.0, 9.4, 18.8, and 37.5 mm/s for venules, small veins, arterioles, and small arteries, respectively (36). Thus, based on blood velocity, it is expected that arterial blood has greater D* than venous blood. Additionally, the pseudo-diffusion phenomenon in a vascular network depends on flow characteristics (e.g., plug flow, laminar flow, and turbulence) and the distribution of vessel orientation in the vasculature. Thus, the critical velocity of diffusion-weighting given in Fig. 5a can only be considered an approximate indicator in determining signal attenuation upon diffusion weighting in vivo.

Implications for BOLD-Based fMRI

BOLD-based fMRI techniques are sensitive both to large venous vessels and to capillaries/tissue. Especially with gradient-echo techniques, the BOLD response is sensitive in and around large venous vessels, which can be distant from the neuronally active sites. To improve the spatial localization of fMRI and to understand the source of the fMRI signal, flow-crushing bipolar gradients have been used in several laboratories (3,35,37,38). The flow-crushing gradients typically employed b-values of ~30 s/mm^2 with a maximum b-value of ~600 s/mm^2. In particular, BOLD-based fMRI signals at 1.5 T are almost eliminated by applying a b-value of 30 s/mm^2, suggesting that BOLD fMRI signals at 1.5 T originate from large venous vessels based on the characteristics of flow-crushing gradients. Based on our PFC study, the total venous blood component from all venous vessels would be attenuated by ~1.5% when a b-value of 30 s/mm^2 was applied. In all venous vessels, the volume fraction of large veins is much less than that of small-size venous vessels, including venules (39). Signals from relatively fast-moving spins in large veins will be selectively reduced by bipolar gradients before those from relatively slow-moving spins in venules and capillaries are suppressed, expecting that the BOLD signal contribution from large veins will be minimized even with a small b-value. Thus, our PFC data are not inconsistent with the BOLD signal elimination at 1.5 T with a b-value of 30 s/mm^2. It should be noted that our estimation based on data obtained in anesthetized animals might not apply to humans because pseudo-diffusion coefficients of arterial and venous blood are closely dependent on flow velocities, which differ in conscious humans and anesthetized animals.

Since BOLD contrast arises from the susceptibility difference between deoxygenated blood and its surroundings, changes in venous blood volume and venous oxygenation level determine BOLD signal changes. Thus, only venous blood volume, not total blood volume, affects BOLD signals (2,40). Until now, it has been assumed that relative venous blood volume change equals the relative total blood volume change, which was measured by contrast agent-based methods (8,12) or estimated from relative CBF change using Grubb's CBF-total CBV relationship (9). Based on Grubb's equation and our findings, a 100% increase in CBF induces ~31% total CBV increase. However, venous rCBV change (e.g., 15%) is about half of the total rCBV change (e.g., 31%). An increase in venous blood volume decreases the BOLD signal, while an increase in venous oxygenation level increases the BOLD signal. For a given BOLD signal change, less venous blood volume contribution requires less blood oxygenation level change. Therefore, the venous oxygenation level change calculated from BOLD and total rCBV changes (instead of the venous CBV change) would be overestimated. The overestimation of venous oxygenation level by using total rCBV during neural stimulation results in an underestimation of oxygen consumption change determined from BOLD and CBF/CBV data (41). These problems can be alleviated by replacing the total rCBV change with the venous rCBV change, i.e., approximately 50% of total rCBV change (40).

To apply the relationship between arterial/venous rCBV and rCBF determined under global stimulation to neural activity, it is assumed that the relationships between rCBV and rCBF during focal stimulation and hypercapnia are similar. Indeed, Mandeville et al. (12) reported that is the case. Given the important application of hypercapnia to modeling the BOLD signal and determining oxygen consumption rate changes using BOLD and CBF measurements, further studies are needed to investigate the relationship between arterial/venous rCBV and rCBF during neural stimulation.

CONCLUSIONS

The relationships among CBF, total CBV, arterial and venous CBV changes were measured in the rat brain during hypercapnia. We found that the venous CBV change during hypercapnia contributed 36% of the total CBV change, and the *relative* CBV change in venous blood was ~50% of the *relative* CBV change in the entire blood. Also, the

arterial rCBV increase was 5.3 times that of the venous rCBV, consistent with the ratio measured in vivo by optical microscopy. The relationship between *venous* rCBV changes and CBF can be readily implemented in the existing BOLD models as a correction factor. Therefore, the new findings will provide a quantitative understanding of the hemodynamic changes underlying the BOLD contrast.

ACKNOWLEDGMENTS

The authors thank Dr. In-Young Choi for help in RF probe design, Drs. Marlene Richter, Hellmut Merkle, and Gregor Adriany for hardware support, and Eric Cohen for proofreading the manuscript. S.G.K. is a NAMI Olmsted County Investigator and T.Q.D. is an NIH postdoctoral fellow.

REFERENCES

1. Ogawa S, Lee T-M, Kay AR, Tank DW. Brain magnetic resonance imaging with contrast dependent on blood oxygenation. Proc Natl Acad Sci USA 1990;87:9868–9872.
2. Ogawa S, Menon RS, Tank DW, Kim S-G, Merkle H, Ellermann JM, Ugurbil K. Functional brain mapping by blood oxygenation level-dependent contrast magnetic resonance imaging. A comparison of signal characteristics with a biophysical model. Biophys J 1993;64:803–812.
3. Lee SP, Silva AC, Ugurbil K, Kim S-G. Diffusion-weighted spin-echo fMRI at 9.4 T: microvascular/tissue contribution to BOLD signal changes. Magn Reson Med 1999;42:919–928.
4. Rosen BR, Belliveau JW, Vevea JM, Brady TJ. Perfusion imaging with NMR contrast agents. Magn Reson Med 1990;14:249–265.
5. Majumdar S, Gore JC. Studies of diffusion in random fields produced by variations in susceptibility. J Magn Reson 1988;78:41–55.
6. Moseley ME, White DL, Wang M, Roth K, Dupon J, Brasch RC. Determination of cerebral blood volume using an intravscular MRI contrast agent. In: ASNR Annual Meeting, Orlando, FL, 1989. p 19.
7. Donahue KM, Weisskoff RM, Chesler DA, Kwong KK, Bogdanov AA Jr, Mandeville JB, Rosen BR. Improving MR quantification of regional blood volume with intravascular T1 contrast agents: accuracy, precision, and water exchange. Magn Reson Med 1996;36:858–867.
8. Mandeville JB, Marota JJ, Kosofsky BE, Keltner JR, Weissleder R, Rosen BR, Weisskoff RM. Dynamic functional imaging of relative cerebral blood volume during rat forepaw stimulation. Magn Reson Med 1998; 39:615–624.
9. Grubb J, Raichle ME, Eichling JO, Ter-Pogossian MM. The effects of changes in $PaCO_2$ on cerebral blood volume, blood flow, and vascular mean transit time. Stroke 1974;5:630–639.
10. Martin WR, Powers WJ, Raichle ME. Cerebral blood volume measured with inhaled $C^{15}O$ and positron emission tomography. J Cereb Blood Flow Metab 1987;7:421–426.
11. Hamberg LM, Hunter GJ, Kierstead D, Lo EH, Gilberto Gonzalez R, Wolf GL. Measurement of cerebral blood volume with subtraction three-dimensional functional CT. AJNR Am J Neuroradiol 1996;17:1861–1869.
12. Mandeville JB, Marota JJ, Ayata C, Zaharchuk G, Moskowitz MA, Rosen BR, Weisskoff RM. Evidence of a cerebrovascular postarteriole windkessel with delayed compliance. J Cereb Blood Flow Metab 1999;19: 679–689.
13. Woolsey TA. Neuronal units linked to microvascular modules in cerebral cortex: response elements for imaging the brain. Cereb Cortex 1996;6:647–660.
14. Iadecola C, Yang G, Ebner TJ, Chen G. Local and propagated vascular responses evoked by focal synaptic activity in cerebellar cortex. J Neurophysiol 1997;78:651–659.
15. Akgoren N, Lauritzen M. Functional recruitment of red blood cells to rat brain microcirculation accompanying increased neuronal activity in cerebellar cortex. Neuroreport 1999;10:3257–3263.
16. Duong TQ, Kim S-G. In vivo MR measurements of regional arterial and venous blood volume fractions in intact rat brain. Magn Reson Med 2000;43:393–402.
17. Silva AC, Zhang W, Williams DS, Koretsky AP. Multi-slice MRI of rat brain perfusion during amphetamine stimulation using arterial spin labeling. Magn Reson Med 1995;33:209–214.
18. Le Bihan D, Breton E, Lallemand D, Grenier P, Cabanis E, Laval-Jeantet M. MR imaging of intravoxel incoherent motions: application to diffusion and perfusion in neurologic disorders. Radiology 1986;161:401–407.
19. Stejskal EO, Tanner JE. Spin diffusion measurements: spin echoes in the presence of a time-dependent field gradient. J Chem Phys 1965;42: 288–292.
20. Neil JJ, Ackerman JJH. Detection of pseudodiffusion in rat brain following blood substitution with perfluorocarbon. J Magn Reson 1992; 97:194–201.
21. Lowe KC. Perfluorocarbons as oxygen-transport fluids. Comp Biochem Physiol 1987;87A:825–838.
22. Riess JG, Le Blanc M. Perfluoro compounds as blood substitutes. Angew Chem Int Ed Eng 1978;17:621–634.
23. Dardzinski BJ, Sotak CH. Rapid tissue oxygen tension mapping using ^{19}F inversion recovery echo planar imaging of perfluoro-15-crown-5-ether. Magn Reson Med 1994;32:88–97.
24. Lee S-P, Choi I-Y, Kim S-G. Rapidly switchable RF coil for 19F/1H NMR studies. In: Proc 8th Annual Meeting ISMRM, Denver, 2000. p 1416.
25. Gruetter R. Automatic, localized in vivo adjustment of all first- and second-order shim coils. Magn Reson Med 1993;29:804–811.
26. Tkac I, Starcuk Z, Choi IY, Gruetter R. In vivo 1H NMR spectroscopy of rat brain at 1 ms echo time. Magn Reson Med 1999;41:649–656.
27. Silva AC, Lee S-P, Yang G, Iadecola C, Kim S-G. Simultaneous BOLD and perfusion functional MRI during forepaw stimulation in rat. J Cereb Blood Flow Metab 1999;19:871–899.
28. Herscovitch P, Raichle ME. What is the correct value for the brain–blood partition coefficient for water? J Cereb Blood Flow Metab 1985; 5:65–69.
29. Zhang W, Williams DS, Koretsky AP. Measurement of rat brain perfusion by NMR using spin labeling of arterial water: in vivo determination of the degree of spin labeling. Magn Reson Med 1993;29:416–421.
30. Dixon WT, Sardashti M, Castillo M, Stomp GP. Multiple inversion recovery reduces static tissue signal in angiograms. Magn Reson Med 1991;18:257–268.
31. Neil J, Bosch S, Ackerman JH. An evaluation of the sensitivity of the intravoxel incoherent motion (IVIM) method of blood flow measurement to changes in cerebral blood flow. Magn Reson Med 1994;32:60–65.
32. Tsekos NV, Zhang F, Merkle H, Nagayama M, Iadecola C, Kim S-G. Quantitative measurements of cerebral blood flow in rats using the FAIR technique: correlation with previous iodoantipyrine autoradiographic studies. Magn Reson Med 1998;39:564–573.
33. Iadecola C, Xu X. Nitro-L-arginine attenuates hypercapnic cerebrovasodilation without affecting cerebral metabolism. Am J Physiol 1994; 266:R518–R525.
34. Wei EP, Seelig JM, Kontos HA. Comparative responses of cerebellar and cerebral arterioles to changes in $PaCO_2$ in cats. Am J Physiol 1984;246: H386–388.
35. Zhong J, Kennan RP, Fulbright RK, Gore JC. Quantification of intravascular and extravascular contributions to BOLD effects induced by alteration in oxygenation or intravascular contrast agents. Magn Reson Med 1998;40:526–536.
36. Guyton AC, Hall JE. In: Textbook of medical physiology, 10th ed. Philadelphia: W.B. Saunders; 2000.
37. Song AW, Wong EC, Tan SG, Hyde JS. Diffusion-weighted fMRI at 1.5T. Magn Reson Med 1996;35:155–158.
38. Boxerman JL, Bandettini PA, Kwong KK, Baker JR, Davis TL, Rosen BR, Weisskoff RM. The intravascular contribution to fMRI signal change: Monte Carlo modeling and diffusion-weighted studies in vivo. Magn Reson Med 1995;34:4–10.
39. Johnson PC, ed. Peripheral circulation. New York: John Wiley & Sons; 1978.
40. Kim S-G, Rostrup E, Larsson HBW, Ogawa S, Paulson OB. Determination of relative $CMRO_2$ from CBF and BOLD changes: significant increase of oxygen consumption rate during visual stimulation. Magn Reson Med 1999;41:1152–1161.
41. Kim S-G, Ugurbil K. Comparison of blood oxygenation and cerebral blood flow effects in fMRI: estimation of relative oxygen consumption change. Magn Reson Med 1997;38:59–65.